The effect of physical ageing on the properties of amorphous PEEK

D. J. Kemmish and J. N. Hay
The Department of Chemistry, The University, Birmingham B15 2TT, UK
(Received 13 August 1984; revised 13 November 1984)

Physical ageing rates of poly(aryl-ether-ether-ketone) have been measured, and interpreted as a kinetic effect associated with the glass formation process. The extent of ageing achieved at equilibrium as measured by differential scanning calorimetry is equal to the product of the super-cooling from the quenched glass transition, and the heat capacity difference between the glass and liquid at the transition temperature. Heat capacities of amorphous and crystalline PEEK have been measured. The activation energy of physical ageing is similar in magnitude to that observed for temperature dependence of crystallization under conditions of viscosity control. Ageing is accompanied by a change in mechanical properties, increased tensile yield stress and drawing stress, more localized yielding and a decrease in impact strength. Fracture surfaces show evidence of mixed modes of fracture.

(Keywords: poly(ether ether ketone); physical ageing kinetics; glass transition; heat capacity; mechanical properties; fracture behaviour)

INTRODUCTION

Physical ageing of amorphous polymers has been attributed to the kinetic nature of the glass transition, and is associated with the progressive change of material properties with time as the non-equilibrium cooled glass reverts towards the supercooled liquid[1].

Molecular relaxation times are such that physical ageing is important in a narrow temperature range below the quenched glass transition temperature. Characteristically physical ageing is accompanied by a reduction in free volume[2], a change in creep characteristics[3], an increased yield stress[4] and increased embrittlement of the polymer on impact[5]. These changes mean that there is considerable commercial interest in the phenomenon, and the corresponding structural changes which accompany it.

Poly(aryl-ether-ketones) have attracted much attention as engineering polymers, especially since they have high temperature stability. By suitable choice of cooling rate from above the melting point, both crystalline and amorphous polymers can be produced. Accordingly, the polymers offer an excellent opportunity to study the effect of molecular structure on physical properties.

The present paper considers the properties of amorphous poly(aryl-ether-ether-ketone), PEEK, and the effect of rate of formation of the glass on the mechanical properties, and fracture behaviour.

EXPERIMENTAL

A commercial grade of PEEK was used as supplied by ICI Ltd., Petrochemical and Plastics Division. It had a melt viscosity as measured by capillary rheometer of 0.43 kNS m^{-2} at 400°C, shear rate 10^3 s^{-1}. Gel permeation chromatographic dispersity was 2.3 with weight and number average molecular weights of 3.9 and 1.7×10^4. We are indebted to Dr P. A. Staniland for the gift of the polymer sample and information on its characteristics.

Amorphous sheets, 20 × 20 cm × 1 mm, were moulded at 400°C and 30 MN m^{-2} pressure for 1.5 min, followed by quenching in ice/water. Thicker sheets were also produced but these were not amorphous but crystallized on quenching. The 1 mm thick sheets were amorphous as determined by density, WAXS and d.s.c.

A Perkin-Elmer differential scanning calorimeter, DSC-2, was used to measure the thermal properties of PEEK as described elsewhere. It was interfaced to an Apple-II microprocessor which stored the calorimeter baseline as a function of temperature, and automatically subtracted from calorimeter response to display specific heats as a function of temperature. The interface A/D convertor substantially improved the accuracy of d.s.c. measurement by × 15.

The thermal response was calibrated with the heat of fusion of ultra-pure indium, 28.4 J g^{-1}, and the temperature of the calorimeter from the melting points of indium, zinc and tin.

Tensile tests were carried out on the Minimat Polymer Laboratories Ltd. microscope extensometer attached to a Leitz Epivert polarized light microscope and standard dumbbell shaped specimens. Impact measurements were made with the Charpy test using a Monsanto Impact machine.

RESULTS AND DISCUSSION

Specific heat of amorphous PEEK

Ice/water quenched thin films were amorphous by WAXS, density and d.s.c. A minimum density of 1 264[2] Kg m^{-3} at 293 K was obtained, and a maximum in the heat of crystallization, of 22 J/g, immediately above the glass transition region. This maximum heat of crystallization corresponded with the development of

0032-3861/85/060905-08$03.00

Table 1 Low temperature crystallization

Density degree of crystallinity (%)	Heat of further crystallization ($J.g^{-1}$)
1.4	17.4
4.3	13.9
6.1	10.0
8.9	7.1
10.1	5.4
13.7	2.7
16.9	1.8

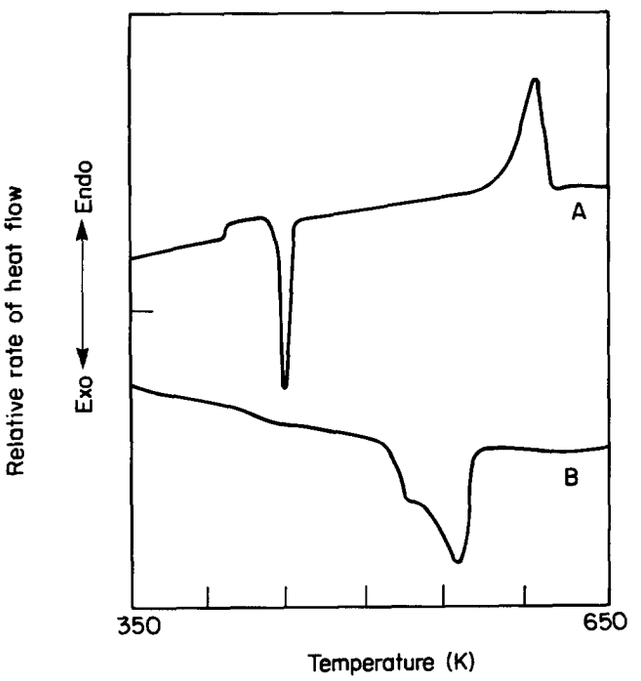

Figure 1 Thermal analysis of PEEK: (A) amorphous on heating; (B) amorphous on cooling

17% crystallinity, as measured by density and X-ray diffraction. The maximum change in specific heat, from the glass to liquid at the quenched glass transition $\Delta C_{p(T_g)}$, was $0.275\,J\,g^{-1}\,K^{-1}$. These measurements were taken as an indication of total amorphous nature of PEEK, and that a standard glass was formed equivalent to quenching at $400\,K\,min^{-1}$.

Amorphous PEEK on heating through the glass transition exhibited a well-defined crystallization exotherm in the region 425–435 K. However, the extent of this crystallization decreased with the initial crystallinity of the specimens, see *Table 1*. Further heating led to more crystallinity developing (annealing) and the subsequent melting above 600 K reflected this further crystallization. Cooling from the melt was followed by re-crystallization in the region 585–600 K, see *Figure 1*. Accordingly, a wide temperature range was available over which PEEK could be crystallized but only narrow gaps in which it crystallized at measurable rates. Crystallization kinetics have been measured[7] in the two regions to produce material of known degrees of crystallinity. However, annealing occurred markedly in low temperature crystallized material and in calibrating the heat of fusion only high temperature crystallized material was used. As reported elsewhere[8] the heat of fusion was $130\,J\,g^{-1}$ and the crystalline density $1{,}378\,Kg\,m^{-3}$. Crystallinities were measured from densities assuming a two-phase system with the amorphous and crystalline densities listed above.

Heat capacities were measured on a range of materials with different degrees of crystallinities, using procedures outlined previously[9,10]. Thermal lags were corrected for, by extrapolating to zero weight. Substantial temperature corrections were involved but experimental variables such as sensitivity, heating rate and sample dimensions had little effect, within the standard error, i.e. ±2%. The quenched samples were initially heated above the glass transition temperature, but below the crystallization temperature, and cooled at a uniform rate. This removed strains within the specimens which gave rise to anomolous 'work' peaks in the glass transition region. All amorphous samples gave identical heat capacity values irrespective of cooling rate, except in the region of the glass transition.

Corrected heat capacities for amorphous PEEK are listed in *Table 2*, outside the glass transition region, crystallization and melting ranges. The heat capacities varied linearly with temperature in the regions, 340–420 K and 600–680 K.

$$C_{AT} = 0.1036 \pm 0.017 + 3.34 \pm 0.05 \times 10^{-3} T\,J\,g^{-1}\,K^{-1} \quad (1)$$

$$C_{AT} = 0.1058 \pm 0.030 + 1.67 \pm 0.05 \times 10^{-3} T\,J\,g^{-1}\,K^{-1} \quad (2)$$

Ageing had no effect on the heat capacities, see *Table 2b*, except in the glass transition region.

The heat capacities of crystalline samples were measured on samples crystallized at 593 K and annealed until 32% crystalline. Assuming a two-phase model for the crystalline polymer, the heat capacity of totally crystalline polymer, $C_{c,T}$, was determined

$$C_{p,T} = (1 - X_c)C_{AT} + X_c C_{cT} \quad (3)$$

for which X_c is the degree of crystallinity. $C_{p,T}$ and $C_{c,T}$ are listed in *Table 2*. Linear plots of $C_{c,T}$ against temperature were obtained such that for 420–570 K,

$$C_{c,T} = 4.75 \pm 0.10 \times 10^{-3} T - 0.73 \pm 0.01\ J\,g^{-1}\,K^{-1} \quad (4)$$

The measured heat capacity data is summarized in *Figure 2*. For the amorphous samples the change in heat capacity on going through the glass transition, ΔC_p, was $0.275 \pm 0.030\,J\,g^{-1}\,K^{-1}$. The partially crystalline material had a higher glass transition temperature and a reduced ΔC_p value. However, ΔC_p was not reduced in proportion to the crystallinity, i.e. $\Delta C_p = 0.106\,J\,g^{-1}\,K^{-1}$ for 32% crystallinity. Moreover, the calculated heat capacities of 100% crystalline material do not extrapolate to those below the transition region (*Figure 2*). This clearly reflects the reduction in mobility of the amorphous regions by the presence of the crystalline phase, the value of ΔC_p being usually attributed to the increased flexibility of the amorphous phase in moving from glass to liquid, and the extra rotational modes involved.

Physical ageing of PEEK

The observed glass transition temperatures of amorphous polymers generally vary markedly with the logarithm of the cooling rate, but not with heating rate. The glass transition of PEEK quenched in the calorimeter at

Table 2a Heat capacities

(a) Amorphous PEEK

Temperature (K)	Mass of sample (mg)				
	49.46	49.46	24.56	24.56	0
340	1.227	1.227	1.235	1.230	1.238
350	1.264	1.263	1.271	1.266	1.274
360	1.299	1.298	1.306	1.302	1.309
370	1.335	1.332	1.340	1.338	1.344
380	1.367	1.364	1.371	1.370	1.376
390	1.398	1.395	1.402	1.401	1.407
400	1.431	1.426	1.434	1.434	1.439
410			Region of T_g		1.501
420					1.758
430	1.765	1.760	1.768	1.767	1.773
440			crystallized		

(b) Effect of ageing, $\Delta H = 2.3\ J\ g^{-1}$

Temperature (K)	0
340	1.241
350	1.276
360	1.312
370	1.346
380	1.377
390	1.408
400	1.440
410	1.484
420	1.528
	1.794

(c) Crystallized PEEK 32% (crystalline)

Temperature (K)	0	100% crystalline
340	1.233	1.23
350	1.271	1.27
360	1.300	1.30
370	1.336	1.34
380	1.371	1.37
390	1.405	1.41
400	1.475	1.44
410	1.474	1.47
420		
430		
440	1.653	1.36
450	1.680	1.41
460	1.707	1.46
470	1.733	1.50
480	1.760	1.55
490	1.787	1.60
500	1.836	1.65
510	1.840	1.69
520	1.87	1.74
530	1.89	1.79
540	1.92	1.83
550	1.94	1.89
560	1.97	1.93
570	2.00	1.98

(d) Amorphous PEEK

Temperature (K)	0
610	2.08
620	2.09
630	2.11
640	2.13
650	2.14
660	2.16
620	2.18
680	2.20

320°C/min from 420 K was 412.7 ± 0.5 K, as measured from the extrapolated peak onset. Specimens held above the glass transition but below the onset of crystallization were quenched at various rates from 320 to 1 K min^{-1}, but the observed glass transition temperature of the glass so formed did not vary with cooling rate. It was concluded that quenching was not occurring from a sufficiently high temperature to enable the glass to form at the rate of cooling, over a sufficient temperature range. Some equilibration of the liquid was occurring within the glass transition region and this had some effect on the measured transition temperature. Heating outside this temperature range produced crystallization of the PEEK and so it was not possible to measure the cooling rate dependence of the transition temperature and hence an activation energy for the process.

The glass transition of specimens held at various temperatures close to but below the transition temperature exhibited marked endothermic peaks, as seen by d.s.c., on heating through the glass transition, see *Figure 3*. These peaks are characteristic of the familiar overshoot of the glass transition temperature associated with physical ageing. The extent of the endothermic process increases logarithmically with time. The excess enthalpy developed at time t, ΔH_t, was measured from the difference between the standard quenched glass and the aged glass between two fixed temperatures as outlined by others[12].

The maximum enthalpy change, ΔH_{max}, is then,

$$\Delta H_{max} = \Delta C_p(T_g - T_A) = \Delta C_p.\Delta T \qquad (5)$$

corresponding to equilibrium having been achieved at T_A, the ageing temperature. The glass transition of PEEK quenched in the calorimeter at 320 K/min from 420 K could thus be calculated from the measured equilibrium excess enthalpy of ageing (ΔH_{max}) after ageing the sample at 412 K for 72 h. The glass transition temperature found by this method is 415.3 ± 0.5 K and this is the value used in the subsequent calculations. The extent of ageing at time t is then

$\Delta H_t/\Delta C_p.\Delta T$ and the extent unaged $(1 - \Delta H/\Delta C_p.\Delta T)$

decreased logarithmically with time at each ageing temperature, see *Figure 4*. These were used to define a

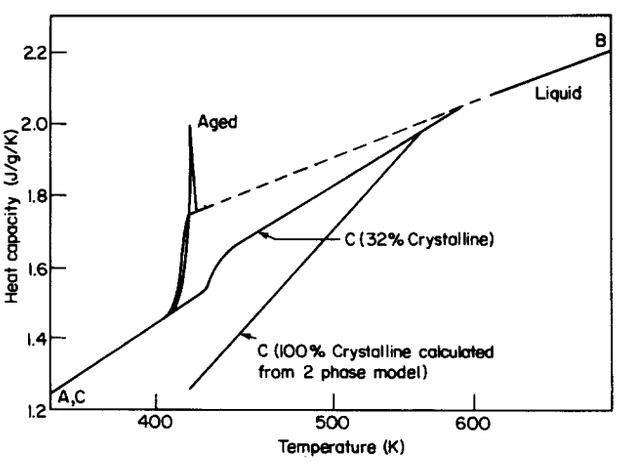

Figure 2 Dependence of heat capacity of PEEK on temperature: (A) glass-amorphous; (B) liquid; (C) crystalline

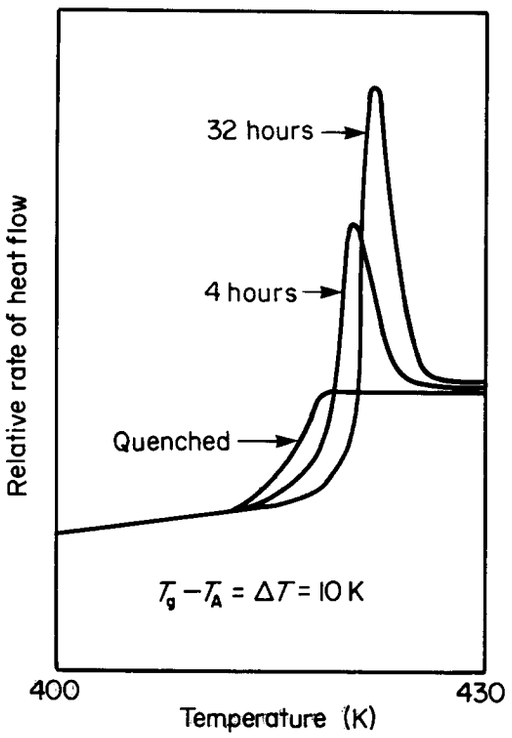

Figure 3 Changing heat capacity with ageing, $\Delta T = T_g - T_A$ the undercooling for glass transition temperatures

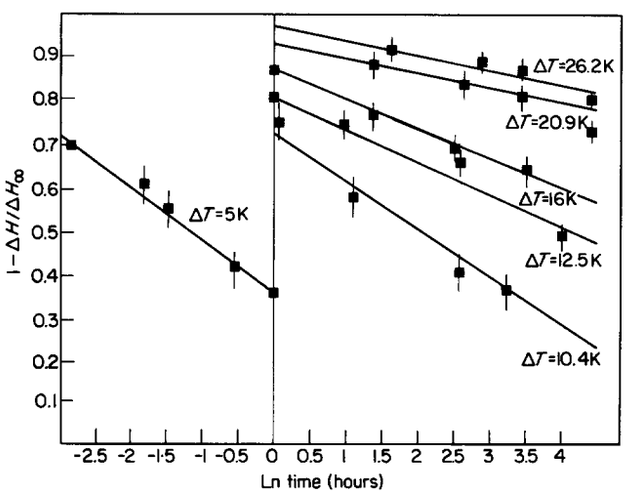

Figure 4 Kinetics of physical ageing. Logarithmic decrease of unaged extent with time

relaxation time, since it has been shown that

$$(1 - \Delta H_t/\Delta C_p.\Delta T) = A \ln\{3/2\, t/\tau\} \qquad (6)$$

An Arrhenius plot of the observed relaxation time, τ, was linear over the limited temperature range of the measurements, see *Table 3*, corresponding to 1.4 ± 0.2 M J mol^{-1}.

Samples of different melt viscosities were also aged over the same temperature range. They, however, aged at the same rate at constant supercooling, ΔT, see *Figure 5*. Molecular weight altered the rate of physical ageing only in changing the glass transition temperature. Kinetic data was superposable by lateral shift along temperature axis equivalent to the change in glass transition. The enthalpy change was equally determined by $\Delta C_p.\Delta T$ and all exhibited the same activation energies within the accuracy of the determination.

Low temperature crystallization

Immediately above the glass transition, PEEK crystallized at increasing rates as the temperature increased, the rate being determined by diffusion rather than nucleation control.

In terms of crystal growth rates, $\dot{g}$, the temperature dependence is determined by the activation energy of mass transfer across the phase boundary, ΔE, and the free energy for formation of the critical size nuclei, ΔG_c^*, i.e.

$$\dot{g} = \dot{g}_0 \exp(-\Delta E/RT) \cdot \exp(-\Delta G_c^*/RT) \qquad (7)$$

At the high degrees of supercooling, growth (and also nucleation) depends only on ΔE, and a measure of ΔE was obtained indirectly from the overall crystallization rate constant, Z, obtained by analysing isothermal crystallization processes with the Avrami equation, i.e.

$$-\ln(1 - x_c) = Zt^n \qquad (8)$$

in which x_c is the degree of crystallinity at time t, and n is a mechanistic constant. Z is a composite rate constant involving both nucleation and growth rate parameters.

D.s.c. was used to analyse the crystallization by heating the quenched glass rapidly to the crystallization temperature. Heat evolution rates were stored as a function of time and the data analysed to determine initial points at which

Table 3 Ageing rate characteristics

Temperature (K)	Relaxation time, τ (hours)	Activation energy (MJ mol^{-1})
411.3	8.2	
404.9	244	
402.8	25.8×10^3	1.4 ± 0.2
399.6	32.1×10^4	
394.4	34.5×10^7	
389.1	31.1×10^{11}	

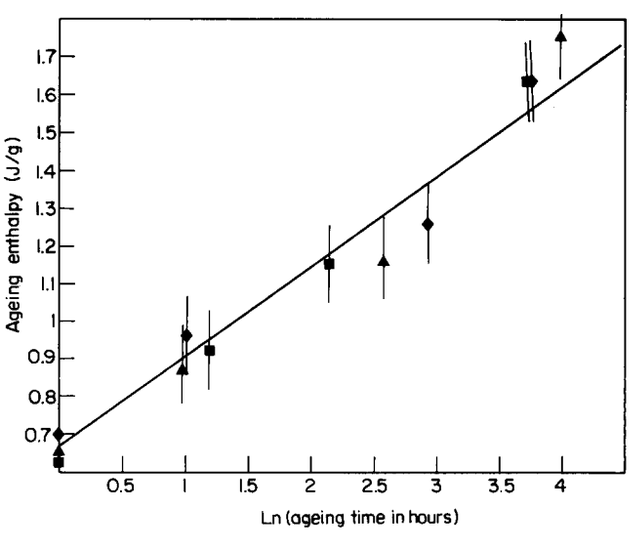

Figure 5 Effect of supercooling and melt viscosity on the rate of physical ageing at $\Delta T = 12.6$ K. (◆) melt viscosity = 0.60; (▲) melt viscosity = 0.45; (■) melt viscosity = 0.21

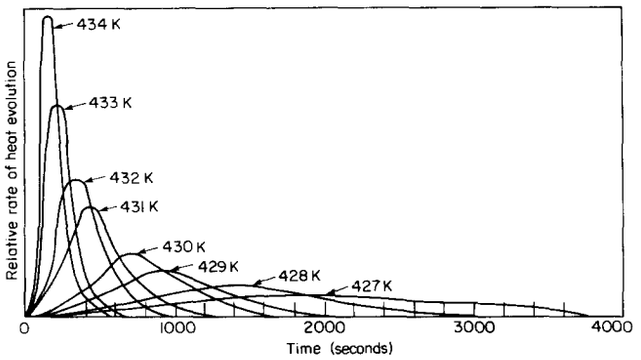

Figure 6 Crystallization rate–time plots for PEEK

Table 4 Isothermal crystallization rate parameters

Temperature (K)	$n_{t_{1/2}}$	$t_{1/2}$ (s)	Z (s^{-3})	Activation energy (MJ mol^{-1})
427.6	2.98±0.10	1980	8.9×10^{-11}	
428.6	2.93	1420	2.4×10^{-10}	
429.6	2.81	990	7.1×10^{-10}	1.35±0.16
430.6	3.10	790	1.9×10^{-9}	
431.6	3.03	480	6.3×10^{-9}	
432.6	3.07	400	1.1×10^{-8}	

sample equilibrated at the crystallization temperature. Initial and final baselines of the calorimeter were determined and subsequently used to determine crystallization heat evolution rate–time dependence. The corrected data were subsequently analysed, re-defining crystallization time from start of crystallization. It was also assumed that the extent of crystallinity which developed at time t, X_t, was

$$X_t = \int_0^t (dH_c/dt)dt \Big/ \int_0^\infty (dH_t/dt)dt \qquad (9)$$

in which dH_c/dt is heat evolution rate at time t, due to crystallization.

Crystallization rates could conveniently be measured from 425–435 K and the rate increased with temperature, see *Figure 6*. Double log plots of $\log(-\ln(1-x_c))$ against $\log t$ were linear initially with slopes equivalent to n. At high conversion, there was a break in the dependence as a secondary process became more important. The primary process was about 80% of the total process. Initial n values were approximately 3.0 consistent with growth of heterogeneously nucleated spherulites. The total kinetic data, and half lives for the crystallization are listed in *Table 4*. An Arrhenius plot of $\log(Z)$ against reciprocal temperature gave an activation energy for mass transfer of 1.35±0.16 M J mol^{-1}.

These samples crystallized close to the glass transition had a limited degree of crystallinity, usually less than 17%, but this could be increased by annealing at higher temperatures.

Mechanical properties of PEEK

Both crystallizing and physical ageing had marked effects on the engineering stress–strain behaviour of PEEK, see *Figure 7*.

On ageing, there was a progressive increase in yield stress from 59 M Pa for the quenched material to as high as 75 M Pa, and a change in elastic modulus. Samples also formed necks indicating drawing stresses changing from 44 to 55 M Pa, and draw ratio also increasing. There was a marked increase in the rate of fall in stress on yielding (geometric strain softening) with ageing. This was evidently associated with the initial formation of localised necks forming at 90° to draw direction in aged specimens. Slip bands were diffused in quenched PEEK forming at about 45° to tensile draw direction at the initial point of neck formation.

The yield stress, σ_y, varied with cross-head speed, and strain rate, $\dot{\varepsilon}$, but the dependence varied markedly with extent of ageing, see *Table 5a*. This is consistent with a

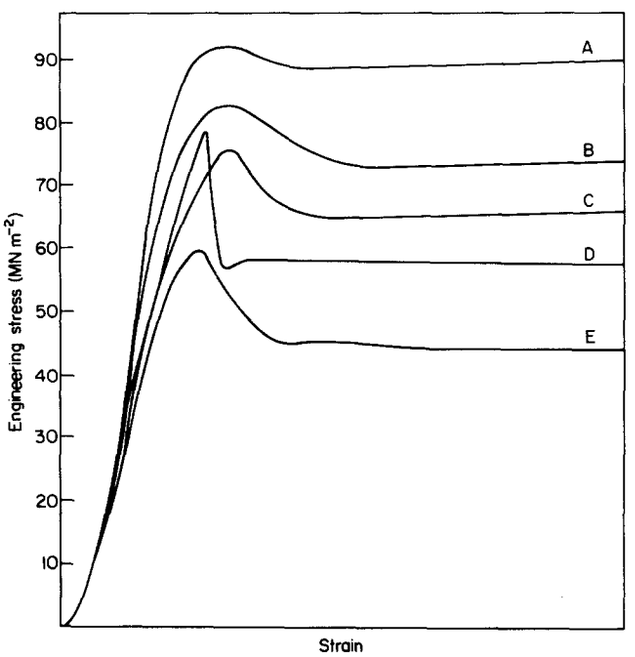

Figure 7 Engineering stress–strain profiles of PEEK: (A) 32% crystalline; (B) 25% crystalline; (C) 15% crystalline; (D) physically aged $\Delta T = 10$ K, for 1 week; (E) quenched amorphous

Table 5 Change in mechanical properties on ageing

(a) Tensile properties

Ageing enthalpy ($J.g^{-1}$)	Yield stress (MPa)	Draw stress (MPa)	Draw ratio
0	59.2	43.8	1.70
0.75	66.2	47.3	
1.38	69.3	48.7	
1.76	71.2	50.2	
2.30	75.1	55.1	2.25

(b) Activation volume for yielding

Sample	Activation volume (nm^3)	Yield stress[a] (MPa)
Quenched	12.6±3.0	59±1
Aged[b]	10.8±2.0	78±1
Crystalline (25%)[c]	9.0±2.0	82±1
Crystalline (32%)	8.6±1.4	90±1

[a] Strain rate 2×10^{-4} s
[b] Aged ΔT 10 K/114 h
[c] Crystallized 428 K and annealed 473/18 h
[d] Crystallized from the melt

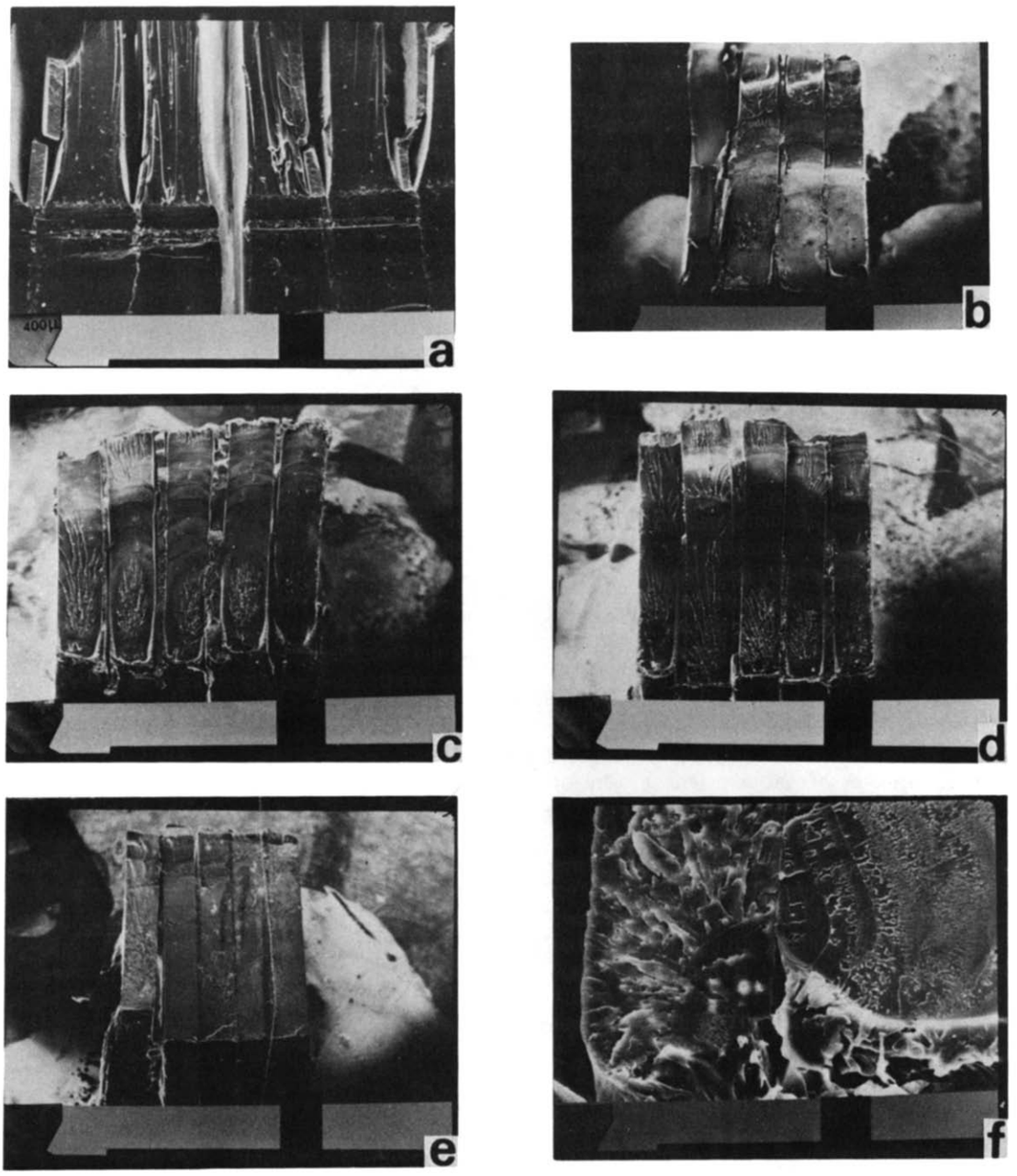

Figure 8 Fracture surface of amorphous, aged and crystalline PEEK laminates: (a) amorphous; (b) aged; (c) 7% crystalline; (d) 15% crystalline; (e) 30% crystalline; (f) brittle fracture in amorphous PEEK initiated by a craze in the glue layer

changing activation volume for the yielding process, i.e. in terms of the Eyring relationship, the activation volume v is

$$v = 4\,kT(\delta \ln \dot{\varepsilon}/\delta\sigma_y) \qquad (10)$$

see *Table 5b*.

Crystallization also substantially increased the yield stress but the neck which formed became progressively more diffuse such that at about 30% crystallinity the material appears to draw uniformly. It was possible to match the increased yield stress on ageing by crystallizing to about 16% crystallinity but the neck profile of the two PEEK specimens were substantially different. The partially crystalline PEEK samples could also be aged below glass transition temperature with a further increase in yield stress and increase in rate of geometric strain softening and localized slip bands. These properties changes are closely associated with ageing, and not the increased yield stress alone.

The ageing endotherm measured by d.s.c. disappeared on yielding aged specimens. Although the yielded material was still amorphous the orientation increased the crystallization rates once the same had been heated above the glass transition temperature. The increased yield stress on ageing implied more mechanical work was involved in deforming aged rather than quenched samples, and that some part of this was associated with the destruction of the ageing.

The additional mechanical work, Δw, was

$$\Delta w = [\sigma_a(\Delta_a - 1) - \sigma_q(\Delta_q - 1)]\rho^{-1} \qquad (11)$$

in which σ_a, σ_q and Δ_a, Δ_q are the drawing stresses and draw ratios of aged and quenched PEEK respectively. ρ is

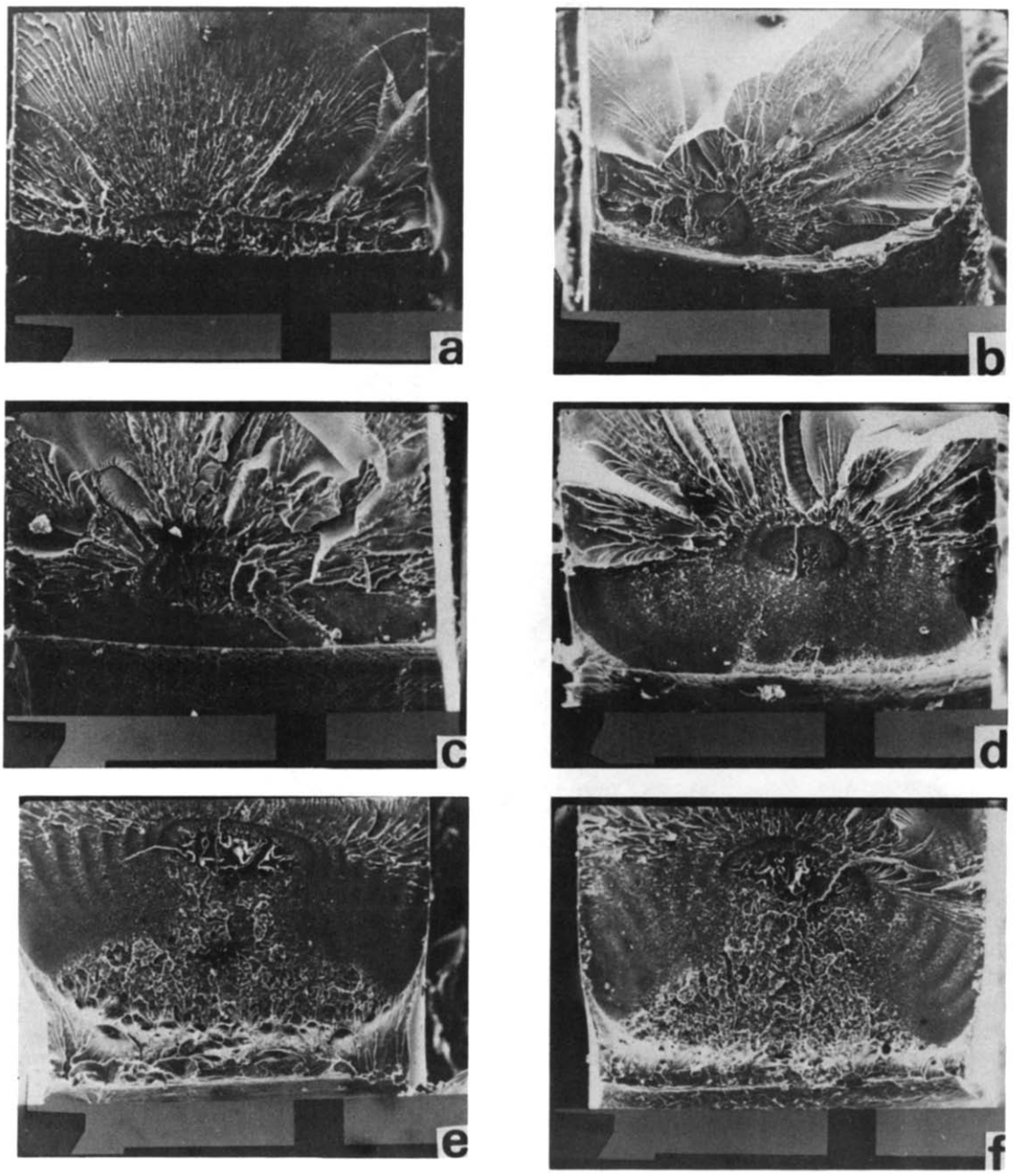

Figure 9 Fracture surfaces of 20% crystalline plaques. Effect of notch-tip radius on fracture mechanism: (a) razor notch; (b) notch tip radius 0.25 mm; (c) 0.5 mm; (d) 1.00 mm; (e) 1.50 mm; (f) 2.00 mm

the density. Draw ratio varied with ageing from 1.70 to 2.25. However, the additional work involved in yielding, 33 J g^{-1}, was substantially larger than ageing enthalpy, 2.67 J g^{-1}, as to imply that the additional mechanical work was not used solely to destroy ageing.

Fracture behaviour of PEEK

Samples of PEEK, thicker than 1 mm, could not be quenched without crystallization occurring. Thin specimens, less than 1 mm thick, did not fracture on impact in Charpy test-rig but flexed out of the retaining supports. In order to obtain some estimate of the impact behaviour of PEEK, laminates of the 1 mm sheets held together with poly(α-cyanoacrylate) adhesive was impacted with various notch tip radii. Even with razor notched specimens the samples were ductile, fracture toughness 85 k J m^{-2} while on ageing or crystallization this dropped to less than a tenth of this value, see *Table 6*.

The fracture surface of the Charpy impact specimens showed evidence of mixed fracture modes in both quenched and aged materials but participating to different extents. The quenched samples showed evidence of plastic deformation with a marked 'pop-in' of the laminate surfaces, and clear evidence of ductile tearing on the surface, see *Figure 8*. Aged specimens showed little or no surface deformation (straight edges between the laminate sheets) with a craze site close to the notch surface. There is a ductile/brittle transition on progressive ageing associated with a change from plane strain to plane stress. Similar effects have been observed previously with PC[5], PVC and PET on ageing and on changing sample dimensions, and increased yield stress. This has been quantified by Parvin and Williams[13] in terms of two fracture toughness parameters associated with plane strain and plane stress conditions, i.e. K_{1c} and K_{2c},

$$K_{obs} = K_{1c} + K_{2c}^2(K_{2c} - K_{1c})/\pi\sigma_y^2 H \qquad (12)$$

Table 6 Impact behaviour

(a) Laminates—Poly α-cyanoacrylate adhesive razor notched specimens

Sample	Impact strength (kJ m^{-2})	Comment
Amorphous—quenched	85	Ductile fracture
aged	7.3	Brittle fracture
Crystalline 7%	5.6	Brittle fracture
15%	2.4	Brittle fracture
25%	2.5	Brittle fracture
30%	3.0	Brittle fracture

(b) 3 mm plaques (supplied by ICI Ltd.)

20% crystalline Notch tip radius (mm)	Impact strength (kJ m^{-2})
Razor	3.5
0.25	5.9
0.50	11
1.00	24
1.50	48
2.00	87

such that the change in yield stress, σ_y, on ageing alone is sufficient to account for the ductile/brittle transition.

Similar changes, see *Figure 9*, were observed in moulded plaques of PEEK (20% crystalline) which could not be attributed to the adhesive. Ductile behaviour is observed with blunt notches (high notch-tip radii) changing progressively towards brittle behaviour with razor notched specimens. Fracture surfaces showed evidence of this change from plane strain to plane stress conditions, and competition between the two mechanisms in that as the notch radius decreases the craze site moves progressively closer to notch surface and there is less surface deformation. Similar observations have been observed with PET.

CONCLUSIONS

Amorphous PEEK ages in an analogous fashion to other polymers, observed previously, and is associated with the kinetic nature of glass transition process. The extent of ageing is related to the supercooling from the glass transition and the change in heat capacity between the glass and the liquid at the transition temperature. The activation energy of the ageing process was the same as that observed for the temperature dependence of the crystallization, under conditions where the onset of the glass transition increases melt viscosity and limits growth. The changes in mechanical and fracture properties on ageing are similar to those observed with PC, and PET and attributed to a change from plane strain to plane stress. There is a ductile/brittle transition.

ACKNOWLEDGEMENTS

We are grateful to the SERC for the award of a CASE award to DJK during the tenure of this work and to industrial collaboration with the International Paint Company Ltd.

REFERENCES

1 Aref-Azar, A., Biddlestone, F., Hay, J. N. and Haward, R. N. *Polymer* 1983, **24**, 1245
2 Illers, K. H. *Makromol. Chem.* 1969, **1**, 127
3 Struik, L. C. E. 'Physical Ageing of Amorphous Polymers and Other Materials', Elsevier, New York and Amsterdam, 1978
4 Adams, G., Cross, A. and Haward, R. N. *J. Mater. Sci.* 1975, **10**, 1582
5 Zurimendi, J. A., Biddlestone, F., Hay, J. N. and Haward, R. N. *J. Mater. Sci.* 1982, **17**, 199
6 Hay, J. N. and Mills, P. J. *Polymer* 1982, **23**, 1380
7 Kemish, D. J. and Hay, J. N., to be published
8 Kemmish, D. J., Hay, J. N., Langford, J. I. and Rae, A. I. M. *Polymer* 1984, **25**, 175
9 Gilmore, I. W. and Hay, J. N. *Polymer* 1977, **18**, 281
10 Hay, J. N. *Polymer* 1978, **19**, 1224
11 Blundell, D. J. and Osborn, B. N. *Polymer* 1983, **24**, 953
12 Savill, N. G. and Richardson, M. J. *Br. Polym. J.* 1979, **11**, 123
13 Parvin, M. and Williams, J. G. *Int. J. Fracture* 1975, **11**, 963